Perspective

Shared Features in Retinal Disorders With Involvement of Retinal Pigment Epithelium

Janet R. Sparrow,[1,2] Rait Parmann,[1] Stephen H. Tsang,[1,2] Rando Allikmets,[1,2] Stanley Chang,[1] and Ruben Jauregui[1]

[1]Department of Ophthalmology, Harkness Eye Institute, Columbia University, New York, New York, United States
[2]Department of Pathology and Cell Biology, Columbia University Medical Center, New York, New York, United States

Correspondence: Janet R. Sparrow, Department of Ophthalmology, Columbia University, New York, NY, 10032, USA; jrs88@columbia.edu.

Received: March 26, 2021
Accepted: May 21, 2021
Published: June 11, 2021

Citation: Sparrow JR, Parmann R, Tsang SH, Allikmets R, Chang S, Jauregui R. Shared features in retinal disorders with involvement of retinal pigment epithelium. *Invest Ophthalmol Vis Sci.* 2021;62(7):15. https://doi.org/10.1167/iovs.62.7.15

When using spectral domain optical coherence tomography (SD-OCT) to inform the status of outer retina, we have noted discrete hyperreflective lesions extending through photoreceptor-attributable bands that have a similar presentation in multiple retinal diseases. These lesions present as either corrugated thickenings of interdigitation zone and ellipsoid zone bands or in later stages as rectangular or pyramidal shaped foci that extend radially through photoreceptor cell-attributable bands. In *ABCA4*-related and *peripherin-2/RDS*-disease (*PRPH2/RDS*), monogenic forms of retinopathy caused by mutations in proteins expressed in photoreceptor cells, these punctate lesions colocalize with fundus flecks in *en face* images. In fundus albipunctatus and retinitis punctata albescens, diseases caused by mutations in genes (*retinol dehydrogenase 5*, *RDH5*; and *retinaldehyde-binding protein 1*, *RLBP1*) encoding proteins of the visual cycle, these lesions manifest as white dot-like puncta. Similar aberrations in photoreceptor cell-attributable SD-OCT reflectivity layers manifest as reticular pseudodrusen (RPD) in short-wavelength fundus autofluorescence and near-infrared fundus autofluorescence fundus images and are linked to age-related macular degeneration a complex disease. Despite differences in the etiologies of retinal diseases presenting as fundus flecks, dots and RPD, underlying degenerative processes in photoreceptor cells are signified in SD-OCT scans by the loss of structural features that would otherwise define healthy photoreceptor cells at these foci.

Keywords: fundus autofluorescence, spectral domain optical coherence tomography, retina, retinal pigment epithelium, retinal disorder, scanning laser ophthalmoscopy, flecks, white-dots, reticular pseudodrusen

Precise phenotyping is crucial to a diagnosis of retinal disorders and to the appropriate selection of patients for clinicals studies designed to evaluate treatment efficacy. To this end, multi-modal fundus imaging technologies have greatly facilitated improved understanding of the natural histories of various retinal diseases.[1,2] A combination of imaging modalities can overcome the limitations of single approaches and can expand the scope of information that can be acquired. Spectral domain optical coherence tomography (SD-OCT) enables noninvasive visualization of normal and pathological retina and is a standard diagnostic tool in clinical ophthalmological diagnosis. The high-resolution images afforded by SD-OCT make it possible to discern multiple hyperreflective bands in human outer retina. Accordingly, SD-OCT has enabled fundamental insights into retinal disease processes including those impacting photoreceptor and retinal pigment epithelial (RPE) cells. For instance, in retinitis pigmentosa, termination of the hyperreflective ellipsoid zone (EZ) is used to identify the boundary between healthy and degenerated photoreceptor cells under conditions of centripetal disease progression.[1,3,4] Intactness of the external limiting membrane (ELM) and EZ is also a strong predictor of visual improvement in eyes undergoing surgery for diabetic macular edema[5] whereas in the setting of geographic atrophy, photoreceptor cell degeneration is connoted by loss of integrity of the ELM and EZ and by thinning of the outer nuclear layer (ONL).[6]

Hyperreflective focal lesions that incorporate photoreceptor-attributable bands in SD-OCT images are features of some retinal diseases of varying etiology (Table). Among these are two monogenic diseases associated with white dot-like fundus lesions caused by mutations in genes encoding proteins of the visual cycle *retinol dehydrogenase 5* (*RDH5*) and *retinaldehyde-binding protein 1* (*RLBP1*).[7–13] Also included in this group are two retinopathies associated with disease variants in *ATP Binding Cassette Subfamily A Member 4* (*ABCA4*) and *peripherin-2/retinal degeneration slow* (*PRPH2/RDS*); both disorders present with fundus flecks.[2,14–22] The correlates of fundus patterning recognized as reticular pseudodrusen (RPD) in AMD also take the form of hyperreflective foci that extend radially through photoreceptor cell-attributable bands in SD-OCT scans.[23–30]

Comparisons amongst white dots, flecks and RPD have not previously been considered yet structural correlates could provide insight into underlying disease mechanisms. Here we will visit similarities and differences in the fundus presentation of these lesions when viewed by near-infrared fundus autofluorescence (NIR-AF) that translates a signal

Table. Multimodal Imaging: Shared Features of Interest

Clinical/Genetic Diagnosis		Expression of Protein Product	Presentation in SD-OCT Scans	Foci Presenting in En Face Images	SW-AF Signal at Foci Relative to Surround	NIR-AF Signal at Foci Relative to Surround
Retinitis punctata albescens	*RLBP1*	RPE	Radial progression of hyperreflective thickening of IZ, EZ; interruption of EZ and ELM; thinning of ONL	Dots	Bright	Dark center with bright surround
Fundus albipunctatus	*RDH5*	RPE		Dots	Bright	Dark center with bright surround
Recessive Stargardt disease	*ABCA4*	Photoreceptors		Flecks	Bright	Reduced or occasionally increased
Pattern dystrophy	*PRPH2/RDS*[§]	Photoreceptors		Flecks	Bright	Reduced or increased
RPD/AMD	Complex	—		RPD	Dark center with bright surround	Dark center with bright surround

EZ, ellipsoid zone; IZ, interdigitation zone.

from melanin, short-wavelength fundus autofluorescence (SW-AF) originating in bisretinoid lipofuscin, and SD-OCT. In one case ultrawide-field pseudocolor fundus images are included. By way of illustrating the structural features of interest we present representative images together with references to the literature. We suggest that an element common to these lesions is the involvement of RPE in the pathological processes and in establishing the fundus patterning. We also propose that these lesions are the products of degenerative processes in photoreceptor cells that are preceded by RPE dysfunction.

White Dot-Like Lesions Associated With Deficiencies in the Visual Cycle

Fundus characteristics associated with mutations in both *RLBP1*/CRALBP and *RDH5* are recognized in color fundus photographs[7,8,10,11] by the presence of numerous discrete white dot-like lesions. Hence, in the ultrawide-field pseudocolor fundus photograph shown here (Figs. 1A, 1B), lightly pigmented puncta are prominently visible in peripheral fundus where they are organized within radial arrays of contrasting pigmentation. This pattern is established by RPE and is similar to the pattern of alternating pigmented and non-pigmented RPE cell clones detected in carriers of ocular albinism due to mutations in *GPR143/OA1*.[31,32] The near-infrared fluorescence signal from melanin is also reduced (Figs 1C, 2A, 3A).

The protein product of *RLBP1 (*cellular retinaldehyde binding protein [CRALBP]) and the protein (11-*cis*-retinaldehyde dehydrogenase) encoded by *RDH5* are both expressed in RPE cells where they function in the visual cycle to promote regeneration of 11-*cis*-retinaldehyde.[33] Accordingly, we have demonstrated here (Figs. 2B, 3B) and previously[34,35] that SW-AF intensities are reduced in patients carrying disease-causing variants in *RLBP1* and *RDH5*. Against the background of hypoautofluorescence, a fine granular autofluorescence is visible centrally in SW-AF images acquired from patients diagnosed with *RLBP1*/CRALBP-associated and RDH5-associated disease (Figs. 2, 3). Target-like configurations presenting as a center and surround of contrasting intensities, are distinctly visible in the pseudocolor (Fig. 1B), NIR-AF (Figs. 1C, 2A, 3A) and SW-AF images (Figs. 2B, 3B) in both *RLBP1*/CRALBP-associated and RDH5-associated disease.

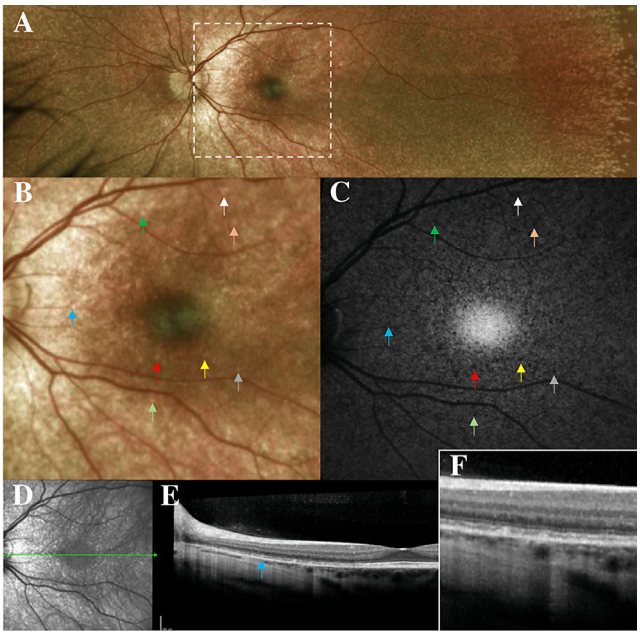

Figure 1. Multimodal fundus images acquired from an adolescent patient (age 15 years) carrying compound heterozygous mutations in *RLBP1* the gene encoding CRALBP. (**A**) Ultrawide-field pseudocolor fundus image. Optos 200 Tx, Optomap Daytona; Optos, Dunfermline, UK; 532 nm green and 633 nm red laser light. Note depigmented white-dot lesions in temporal retina. (**B**) Magnification of area outlined in A. (**C**) Near-infrared fundus autofluorescence (NIR-AF; 787 nm) image. Examples of corresponding lesions are indicated by color-coded arrows. (**D, E**) Infrared reflectance (IR-R; **D**) and SD-OCT **(E)** images. The horizontal axis of the scan in **E** is shown in **D**. (**F**) Magnification of area in **E**.

Aberrations in the SD-OCT scans correspond to the dots observed in the en face images (Fig. 1D).[12] As shown in Figures 1 and 2, the SD-OCT images acquired from the patients carrying mutations in *RLBP1* reveal multiple hyper-

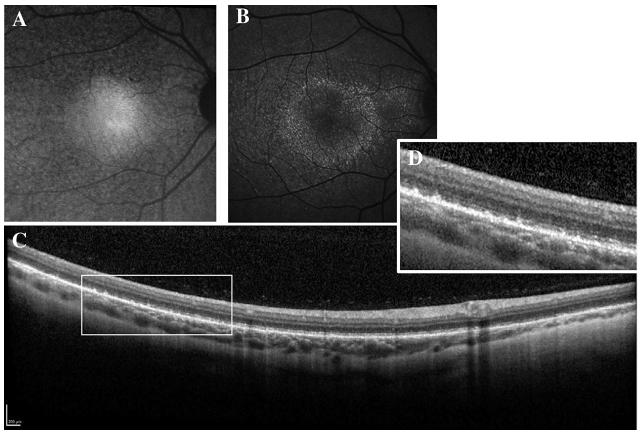

Figure 2. Fundus images of a 13-year-old patient carrying compound heterozygous mutations in *RLBP1*. (**A**) NIR-AF image (787 nm). (**B**) SW-AF (488 nm). Depigmented foci are dark in NIR-AF and SW-AF images. (**C**) SD-OCT scan. (**D**) Magnification of area in **C**. Images are representative of two patients.

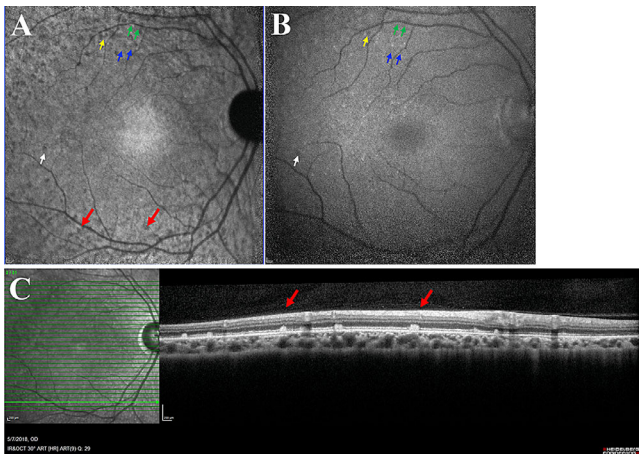

Figure 3. Fundus images obtained from a patient (age 14 years) exhibiting mutations in *RDH5*/11-cis-retinol dehydrogenase. (**A**) NIR-AF (787 mm). (**B**) SW-AF (488 nm). *Arrows* are color-coded (*yellow*, *green*, *blue*, *white*) to indicate corresponding lesions visible in the two modalities. Depigmented foci are dark in NIR-AF and SW-AF images. (**C**) SD-OCT (*right*) with IR-R (*left*). The horizontal axis of the SD-OCT image is indicated in the IR-R image by the *green line* ending in an *arrow*. Corresponding foci in **A** and **C** are indicated by *red arrows*. The detectability of the autofluorescent puncta (**B**) in SW-AF images despite RDH5 deficiency and reduced availability of 11-*cis*-retinaldehyde is likely enabled by the use of a higher than typical sensitivity setting; by image processing that enhances contrast by stretching intensity values to span the full grayscale range (0–255); and by reduced signal attenuation by photopigment and melanin.

reflective thickenings of the IZ along with altered contours of the EZ (Figs. 1E, 2C). In the case of RDH5-associated disease as shown in Figure 3C, outer photoreceptor-attributable bands in the SD-OCT images present with numerous well demarcated dome-or rectangular-shaped outer retinal lesions extending from the RPE through reflectivity bands attributable to the outer and inner segments of photoreceptor cells. At these foci the ELM is interrupted and ONL Is often thinned. Hypertransmission of SD-OCT signal, indicative of widespread RPE cell defects in extrafoveal retina is pronounced with *RLBP1*-mutations

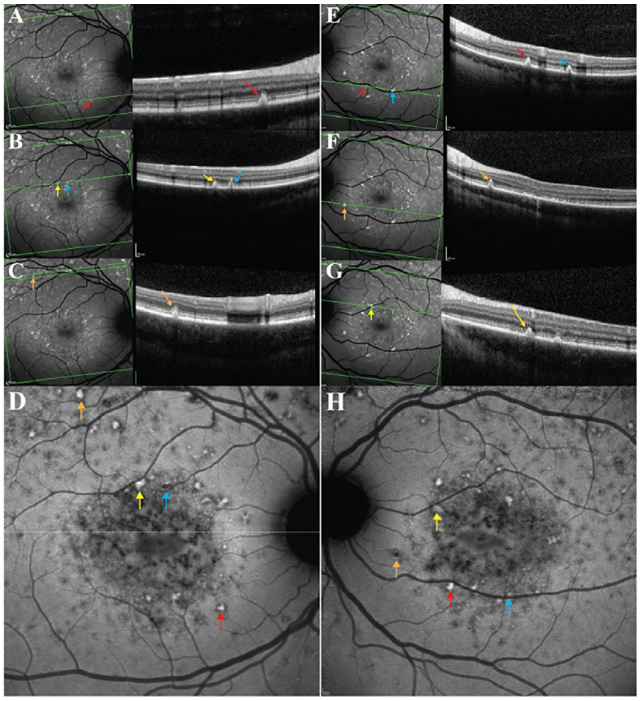

Figure 4. Representative fundus images of flecks in recessive Stargardt disease. Patient age 14 years. (**A–C**, **E–G**) SW-AF (488 nm) images (*left*) registered to SD-OCT scans (*right*). The horizontal axis of the SD-OCT image is indicated in the SW-AF image by the *green line*. Corresponding flecks in SW-AF and SD-OCT images are indicated by color-coded arrows. (**D**) NIR-AF (787 nm) image of the fundus presented in **A–D**. (**H**) NIR-AF image of the fundus presented in E-G. Flecks in **D** and **H** corresponding to the flecks in **A–D** and **E–G** are indicated by *arrows* of the same color. Images are representative of 16 patients (32 eyes).

(Figs. 1E, 1F, 2C). Outer retinal aberrations akin to those described above, together with punctate white dots in the fundus are also features of vitamin A deficiency.[36,37]

Diseases Exhibiting Fundus Flecks

ABCA4-related and *PRPH2/RDS*-associated diseases are, respectively, autosomal recessive and autosomal dominant forms of inherited retinopathies. In both cases, the disease-causing gene is expressed in photoreceptor cells and in both disorders, patients exhibit autofluorescent fundus flecks (Figs. 4A–4C, 4E–4G, 5E).[2,14–21] The ABCA4 protein is involved in the handling of retinaldehyde[38] while PRPH2/RDS plays a key role in the formation of outer segment disks.[39] The brightness of flecks in *ABCA4*-disease is associated with elevated levels of bisretinoid lipofuscin; the latter forms in photoreceptor cells and accumulates in RPE.[40] These fluorophores confer a dark choroid in *ABCA4*-affected patients undergoing fluorescein angiography and are the source of elevated SW-AF. [40–42] Conversely, in the presence of *PRPH2/RDS* mutations a "dark choroid" in fluorescein angiograms is not observed[19] and based on quantitative fundus autofluorescence measurements, SW-AF intensities are only modestly elevated in a subset of patients.[43] Some flecks in both *ABCA4*- and *PRPH2/RDS*-associated diseases are accompanied by a halo of reduced SW-AF (Figs. 4A–4C, 4E–4G, 5E, orange arrow) and central older flecks

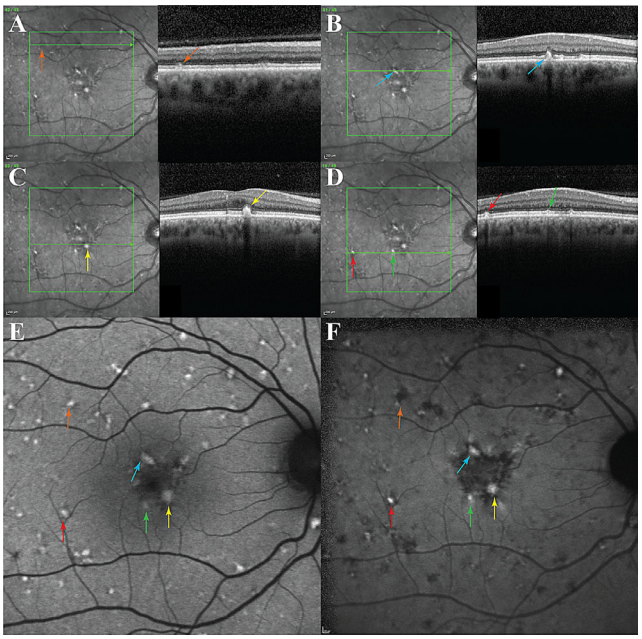

Figure 5. Fundus images presenting disease features characteristic of *PRPH2/RDS*-associated disease. Patient age 36 years (**A–D**). IR-R (*left*) and SD-OCT (*right*) scans. The horizontal axis of the SD-OCT image is indicated in the IR-R image by the green line. Corresponding flecks in IR-R and SD-OCT images are indicated by arrows of the same color. **(E)** Short-wavelength fundus autofluorescence (SW-AF; 488 nm). (**F**) NIR-AF (787 nm). Corresponding flecks in **A** to **F** are indicated by *colored arrows*. Note flecks exhibiting hyperautofluorescence or hypoautofluorescence. Images are representative of seven patients (14 eyes).

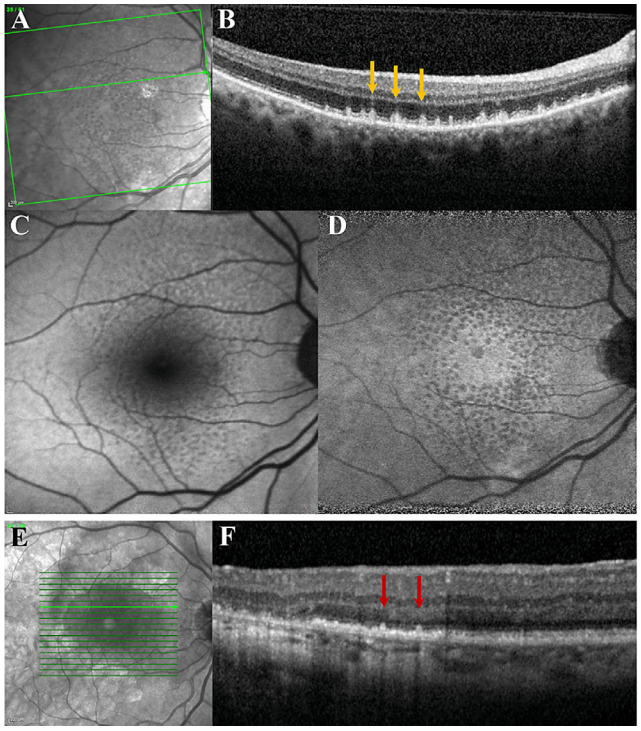

Figure 6. Fundus images of RPD (age 90 years) and L-ORD (age 63 years). (**A**) RPD: IR-R. (**B**) RPD: SD-OCT. (**C**) RPD: SW-AF (488 nm). (**D**) NIR-AF (787 nm). RPD colocalize as darkened foci in SW-AF and NIR-AF and as conical-shaped lesions (*orange arrows*) that extend through the interdigitation zone and ellipsoid zone bands in SD-OCT scans. The central *green line* in **A** indicates the horizontal axis of the SD-OCT scan. RPD images are representative of nine patients (18 eyes). (**E, F**) IR-R (**E**) and corresponding SD-OCT image (**F**) of fundus of patient carrying the single missense variant S163R in CTRP5/C1QTNF5 [c.489C>A); p.(Ser163Arg)] conferring L-ORD.

are entirely hypoautofluorescent in SW-AF images (Figs. 4E–4G, 5E).[16,20,22]

Conversely, the NIR-AF signal originating in melanin at the position of flecks in both *ABCA4*- (Figs. 4D, 4H) and *PRPH2/RDS*-associated disease (Fig. 5F) are more often hypoautofluorescent than hyperautofluorescent, and the profiles are often larger in NIR-AF images than in SW-AF images (Figs. 4H, 5F). In SD-OCT images acquired from individuals having *ABCA4*- and *PRPH2/RDS*-disease, flecks co-localize with hyperreflective barrel- or pyramidal-shaped profiles (Figs. 4A–4C, 4E–4G, 5A–5D). In some cases the hyperreflectivity is limited to thickening of the IZ and EZ whereas in other cases flecks extend anteriorly through the EZ and ELM. ONL thickness decreases as the lesion expands anteriorly and progressively incorporates photoreceptor-attributable SD-OCT bands. Fundus flecks in *ABCA4*-disease have been shown to originate at the level of photoreceptor cells.[20,44] Accordingly, fleck hyperautofluorescence originating from impaired photoreceptor cells in the presence of *PRPH2/RDS* mutations might also explain the relative brightness of the flecks even as retina-wide bisretinoid lipofuscin formation is not increased with *PRPH2/RDS* mutations.

Diseases Presenting With Reticular Fundus Patterns

In SW-AF and NIR-AF images RPD are readily identified as interlacing ribbons, circular or oval foci with darkened centers and a brighter annulus (Figs. 6C, 6D).[25,26,29,45–50] In the en face patterns, the darkened foci in the SW-AF images are similarly darkened in NIR-AF images (Figs. 6C, 6D); the brighter annulus also colocalizes in the two modalities. While in SW-AF images the presence of macular pigment obscures the visibility of RPD in central-most retina, these lesions are readily visible centrally when examined with NIR-AF (Figs. 6C, 6D). RPD lesions visible in fundus images of AMD patients confer increased risk of advanced disease.[24,51–53]

As with white dots and flecks, RPD colocalize with hyperreflective lesions in photoreceptor-attributable SD-OCT bands (Fig. 6B).[25,26,29] These lesions present as either shallow corrugations of IZ and EZ bands that may be indicative of disease beginning in outer segments or at later stages[54] as rectangular, oval or pyramidal shaped foci that extend radially through photoreceptor cell-attributable bands progressively interrupting IZ, EZ, and ELM. RPD are associated with ONL thinning. The SD-OCT lesions corresponding to RPD in SW-AF images do not displace outer retinal layers anteriorly[25,29] as would be expected of extracellular deposits. Hypertransmission of SD-OCT signal into the choroid is observed in connection with some RPD (Fig. 6B)[29,48,54,55]; this feature is indicative of local RPE atrophy in association with these RPD.

The SD-OCT aberrations discussed above are not limited to RPD in the setting of AMD. For instance, reticular patterning is visible in the fundus of patients with late-onset retinal degeneration (L-ORD), an autosomal dominant disorder that

is caused by a p.Ser163Arg point mutation in the complement 1q tumor necrosis factor 5 gene (*CTRP5/C1QTNF5*) that is expressed in RPE and ciliary epithelium.[56–58] Spots of hypoautofluorescence surrounded by halos of slightly brighter autofluorescence in SW-AF images.[13,19,59,60] are considered to be the equivalent of the dot-like sub-type of RPD.

In SD-OCT scans the reticular patterns co-localize with scalloped irregularities of the IZ and EZ reflectivity bands, and in more advanced cases, with conical lesions extending through the EZ line and into the thinner ONL (Figs. 6E, 6F). Both RPD and L-ORD are associated with abnormalities in dark-adaptation and progression to loss of RPE and photoreceptor cells.[30,56,61]

Another example is available from the literature. The undulations and discontinuities of the EZ band observed in SD-OCT scans in association with Sorsby fundus dystrophy have also been likened to RPD.[13,62] In SW-AF images these lesions appear target- or ribbon-like.[62] This autosomal dominant macular dystrophy caused by variants in the gene encoding tissue inhibitor of metalloproteinase-3 (*TIMP3*) leads to RPE cell loss.[63]

Comments

Features of white dots, flecks and RPD lesions suggest that RPE are disabled or atrophied at these positions. For instance, the punctate lesions taking the form of flecks are typically hyperfluorescent in fluorescein angiograms in association with *PRPH2/RDS*-associated disorders.[19] White dot lesions associated with mutations in *RLBP1* are also hyperfluorescent in fluorescein angiograms.[64] These window defects indicate that the RPE monolayer is not fully intact. Also indicative of a breach in the RPE monolayer is evidence of hypertransmission of OCT signal into the choroid. RPD in AMD are often but not always associated with increased transmission of OCT signal into the choroid.[29,48,54,55]

Flecks in association with disease variants in *ABCA4* or *PRPH2/RDS* can be associated with hypertransmission into the choroid or the fleck can cast a shadow[2,22]; the latter may be due to screening by elevated fluorophore concentrations in the outer segments. In the presence of *RLBP1*/CRALBP and *RDH5* mutations hypertransmission is widespread (Figs. 1–3). Reduced NIR-AF intensities in patients diagnosed with *RDH5*, and *RLBP1/CRALBP*-related disease[34] are also suggestive of thinned or atrophied RPE. NIR-AF signal is substantially reduced at many but not all fleck loci in *ABCA4*- and *PRPH2/RDS*-associated diseases (Figs. 4, 5) whereas RPD in SD-OCT scans colocalize with NIR-AF that is reduced but not absent. Reduced NIR-AF signal suggests a reduction in melanin that could be accounted for by RPE thinning. With regard to alternative interpretations, we note that the reduced NIR-AF signal is unlikely to be due to absorption by tissue anterior to the lesion. For instance, as noted above, increased transmission of signal into the choroid can be observed in SD-OCT scans in the presence of flecks, dots and RPD and in some cases the NIR-AF of flecks is even increased (Fig. 4).

Final Thoughts

In many forms of RP, mutations in photoreceptor-specific genes leads to retinal degeneration with widespread death of rods and cones.[65–69] Yet orderly photoreceptor cell degeneration proceeds without the formation of punctate lesions in en face images nor the presence of intermittent hyperreflective foci in SD-OCT scans. Conversely, in other retinal diseases of varying etiology, photoreceptor cell-attributable bands in SD-OCT scans are interrupted intermittently by hyperreflective focal lesions. We suggest that in diseases associated with flecks, white-dots and RPD, the hyperreflective focal aberrations visible in SD-OCT scans represent degenerative changes in groups of photoreceptor cells secondary to disease processes in the underlying RPE. The hyperreflective shallow corrugations observed in the IZ and EZ bands of SD-OCT scans may be indicative of disease beginning in outer segments. These disease processes can arise because of mutations in genes whose protein product is expressed in photoreceptor cells (*ABCA4*/STGD1; *PRPH2*/RDS) yet severely impact RPE. In other cases the mutated genes are expressed in RPE (*RLBP1*/CRALBP and *RDH5*). Just as the hyperautofluorescent fundus rings in RP track the progress of photoreceptor cell degeneration, flecks, white-dots and RPD may signify photoreceptor cell degeneration in some retinal diseases involving RPE. Additional studies are warranted to determine whether the rate at which the punctate lesions extend radially and the frequency of the lesions at any given time are determined by genetic factors.

Acknowledgments

Supported in part by grants from the National Eye Institute/NIH EY024091 and P30 EY019007, Foundation Fighting Blindness, Jonas Children's Vision Care and a grant from Research to Prevent Blindness to the Department of Ophthalmology, Columbia University.

Disclosure: **J.R. Sparrow,** None; **R. Parmann,** None; **S.H. Tsang,** None; **R. Allikmets,** None; **S. Chang,** None; **R. Jauregui,** None

References

1. Cabral T, Sengillo JD, Duong JK, et al. Retrospective analysis of structural disease progression in retinitis pigmentosa utilizing multimodal imaging. *Sci Rep*. 2017;7:10347.
2. Duncker T, Marsiglia M, Lee W, et al. Correlations amongst near-infrared and short-wavelength autofluorescence and spectral domain optical coherence tomography in recessive Stargardt disease. *Invest Ophthalmol Vis Sci*. 2014;55:8134–8143.
3. Birch DG, Locke KG, Wen Y, Locke KI, Hoffman DR, Hood DC. Spectral-domain optical coherence tomography measures of outer segment layer progression in patients with X-linked retinitis pigmentosa. *JAMA Ophthalmol*. 2013;131:1143–1150.
4. Tee JJL, Carroll J, Webster AR, Michaelides M. Quantitative analysis of retinal structure using spectral-domain optical coherence tomography in RPGR-associated retinopathy. *Am J Ophthalmol*. 2017;178:18–26.
5. Chhablani JK, Kim JS, Cheng L, Kozak I, Freeman W. External limiting membrane as a predictor of visual improvement in diabetic macular edema after pars plana vitrectomy. *Graefes Arch Clin Exp Ophthalmol*. 2012;250:1415–1420.
6. Guymer RH, Rosenfeld PJ, Curcio CA, et al. Incomplete retinal pigment epithelial and outer retinal atrophy in age-related macular degeneration: classification of Atrophy Meeting Report 4. *Ophthalmology*. 2020;127:394–409.
7. Sergouniotis PI, Sohn EH, Li Z, et al. Phenotypic variability in RDH5 retinopathy (Fundus Albipunctatus). *Ophthalmology*. 2011;118:1661–1670.

8. Wang C, Nakanishi N, Ohishi K, et al. Novel RDH5 mutation in family with mother having fundus albipunctatus and three children with retinitis pigmentosa. *Ophthalmic Genet*. 2008;29:29–32.
9. Burstedt M, Jonsson F, Kohn L, Burstedt M, Kivitalo M, Golovleva I. Genotype-phenotype correlations in Bothnia dystrophy caused by RLBP1 gene sequence variations. *Acta Ophthalmol*. 2013;91:437–444.
10. Burstedt MS, Forsman-Semb K, Golovleva I, Janunger T, Wachtmeister L, Sandgren O. Ocular phenotype of Bothnia dystrophy, an autosomal recessive retinitis pigmentosa associated with an R234W mutation in the RLBP1 gene. *Arch Ophthalmol*. 2001;119:260–267.
11. Genead MA, Fishman GA, Lindeman M. Spectral-domain optical coherence tomography and fundus autofluorescence characteristics in patients with fundus albipunctatus and retinitis punctata albescens. *Ophthalmic Genet*. 2010;31:66–72.
12. Querques G, Carrillo P, Querques L, Bux AV, Del Curatolo MV, Delle Noci N. High-definition optical coherence tomographic visualization of photoreceptor layer and retinal flecks in fundus albipunctatus associated with cone dystrophy. *Arch Ophthalmol*. 2009;127:703–706.
13. Khan KN, Mahroo OA, Khan RS, et al. Differentiating drusen: drusen and drusen-like appearances associated with ageing, age-related macular degeneration, inherited eye disease and other pathological processes. *Prog Retin Eye Res*. 2016;53:70–106.
14. Eagle RC, Lucier AC, Bernardino VB, Yanoff M. Retinal pigment epithelial abnormalities in fundus flavimaculatus. *Ophthalmology*. 1980;87:1189–1200.
15. Westeneng-van Haaften SC, Boon CJ, Cremers FP, Hoefsloot LH, den Hollander AI, Hoyng CB. Clinical and genetic characteristics of late-onset Stargardt's disease. *Ophthalmology*. 2012;119:1199–1210.
16. Cukras CA, Wong WT, Caruso R, Cunningham D, Zein W, Sieving PA. Centrifugal expansion of fundus autofluorescence patterns in Stargardt disease over time. *Arch Ophthalmol*. 2012;130:171–179.
17. Kellner S, Kellner U, Weber BH, Fiebig B, Weinitz S, Ruether K. Lipofuscin- and melanin-related fundus autofluorescence in patients with ABCA4-associated retinal dystrophies. *Am J Ophthalmol*. 2009;147:895–902.
18. Zhang K, Garibaldi DC, Li Y, Green WR, Zack DJ. Butterfly-shaped pattern dystrophy: a genetic, clinical, and histopathological report. *Arch Ophthalmol*. 2002;120:485–490.
19. Boon CJ, van Schooneveld MJ, den Hollander AI, et al. Mutations in the peripherin/RDS gene are an important cause of multifocal pattern dystrophy simulating STGD1/fundus flavimaculatus. *Br J Ophthalmol*. 2007;91:1504–1511.
20. Sparrow JR, Marsiglia M, Allikmets R, et al. Flecks in recessive Stargardt disease: short-wavelength autofluorescence, near-infrared autofluorescence, and optical coherence tomography. *Invest Ophthalmol Vis Sci*. 2015;56:5029–5039.
21. Walia S, Fishman G. Natural history of phenotypic changes in Stargardt macular dystrophy. *Ophthalmic Genet*. 2009;30:63–68.
22. Paavo M, Lee W, Allikmets R, Tsang S, Sparrow JR. Photoreceptor cells as a source of fundus autofluorescence in recessive Stargardt disease. *J Neurosci Res*. 2019;97:98–106.
23. Finger RP, Chong E, McGuinness MB, et al. Reticular pseudodrusen and their association with age-related macular degeneration: the Melbourne Collaborative Cohort Study. *Ophthalmology*. 2016;123:599–608.
24. Finger RP, Wu Z, Luu CD, et al. Reticular pseudodrusen: a risk factor for geographic atrophy in fellow eyes of individuals with unilateral choroidal neovascularization. *Ophthalmology*. 2014;121:1252–1256.
25. Zweifel SA, Imamura Y, Spaide TC, Fujiwara T, Spaide RF. Prevalence and significance of subretinal drusenoid deposits (reticular pseudodrusen) in age-related macular degeneration. *Ophthalmology*. 2010;117:1775–1781.
26. Zweifel SA, Spaide RF, Curcio CA, Malek G, Imamura Y. Reticular pseudodrusen are subretinal drusenoid deposits. *Ophthalmology*. 2010;117:303–312.e301.
27. Domalpally A, Agron E, Pak JW, et al. Prevalence, risk, and genetic association of reticular pseudodrusen in age-related macular degeneration: Age-Related Eye Disease Study 2 Report 21. *Ophthalmology*. 2019;126:1659–1666.
28. Hogg RE, Silva R, Staurenghi G, et al. Clinical characteristics of reticular pseudodrusen in the fellow eye of patients with unilateral neovascular age-related macular degeneration. *Ophthalmology*. 2014;121:1748–1755.
29. Paavo M, Lee W, Merriam J, et al. Intraretinal correlates of reticular pseudodrusen revealed by autofluorescence and en face OCT. *Invest Ophthalmol Vis Sci*. 2017;58:4769–4777.
30. Flamendorf J, Agron E, Wong WT, et al. Impairments in dark adaptation are associated with age-related macular degeneration severity and reticular pseudodrusen. *Ophthalmology*. 2015;122:2053–2062.
31. Schmidt GH, Wilkinson MM, Ponder BA. Non-random spatial arrangement of clone sizes in chimaeric retinal pigment epithelium. *J Embryol Exp Morphol*. 1986;91:197–208.
32. Paavo M, Zhao J, Kim HJ, et al. Mutations in GPR143/OA1 and ABCA4 inform interpretations of short-wavelength and near-infrared fundus autofluorescence. *Invest Ophthalmol Vis Sci*. 2018;59:2459–2469.
33. Saari JC. Vitamin A and vision. *Subcell Biochem*. 2016;81:231–259.
34. Oh JK, Lima de Carvalho JR, Jr., Ryu J, Tsang SH, Sparrow JR. Short-wavelength and near-infrared autofluorescence in patients with deficiencies of the visual cycle and phototransduction. *Sci Rep*. 2020;10:8998.
35. Lima de Carvalho JR, Jr., Kim HJ, Ueda K, et al. Effects of deficiency in the RLBP1-encoded visual cycle protein CRALBP on visual dysfunction in humans and mice. *J Biol Chem*. 2020;295:6767–6780.
36. Apushkin MA, Fishman GA. Improvement in visual function and fundus findings for a patient with vitamin A-deficient retinopathy. *Retina*. 2005;25:650–652.
37. Aleman TS, Garrity ST, Brucker AJ. Retinal structure in vitamin A deficiency as explored with multimodal imaging. *Doc Ophthalmol*. 2013;127:239–243.
38. Quazi F, Molday RS. ATP-binding cassette transporter ABCA4 and chemical isomerization protect photoreceptor cells from the toxic accumulation of excess 11-cis-retinal. *Proc Natl Acad Sci U S A*. 2014;111:5024–5029.
39. Stuck MW, Conley SM, Naash MI. PRPH2/RDS and ROM-1: Historical context, current views and future considerations. *Prog Retin Eye Res*. 2016;52:47–63.
40. Burke TR, Duncker T, Woods RL, et al. Quantitative fundus autofluorescence in recessive Stargardt disease. *Invest Ophthalmol Vis Sci*. 2014;55:2841–2852.
41. Fishman GA, Farber M, Patel BS, Derlacki DJ. Visual acuity loss in patients with Stargardt's macular dystrophy. *Ophthalmology*. 1987;38:809–814.
42. Delori FC, Staurenghi G, Arend O, Dorey CK, Goger DG, Weiter JJ. In vivo measurement of lipofuscin in Stargardt's disease—Fundus flavimaculatus. *Invest Ophthalmol Vis Sci*. 1995;36:2327–2331.
43. Duncker T, Tsang SH, Woods RL, et al. Quantitative fundus autofluorescence and optical coherence tomography in PRPH2/RDS- and ABCA4-associated disease

Investigative Ophthalmology & Visual Science

exhibiting phenotypic overlap. *Invest Ophthalmol Vis Sci*. 2015;56:3159–3170.
44. Greenstein VC, Nunez J, Lee W, et al. A comparison of en face optical coherence tomography and fundus autofluorescence in Stargardt disease. *Invest Ophthalmol Vis Sci*. 2017;58:5227–5236.
45. Mimoun G, Soubrane G, Coscas G. Macular drusen. *J Fr Ophtalmol*. 1990;13:511–530.
46. Fleckenstein M, Issa PC, Helb HM, et al. High-resolution spectral domain-OCT imaging in geographic atrophy associated with age-related macular degeneration. *Invest Ophthalmol Vis Sci*. 2008;49:4137–4144.
47. Sivaprasad S, Bird A, Nitiahpapand R, et al. Perspectives on reticular pseudodrusen in age-related macular degeneration. *Surv Ophthalmol*. 2016;61:521–537.
48. Lee MY, Yoon J, Ham DI. Clinical features of reticular pseudodrusen according to the fundus distribution. *Br J Ophthalmol*. 2012;96:1222–1226.
49. Chan H, Cougnard-Gregoire A, Delyfer MN, et al. Multimodal imaging of reticular pseudodrusen in a population-based setting: The Alienor Study. *Invest Ophthalmol Vis Sci*. 2016;57:3058–3065.
50. Alten F, Clemens CR, Milojcic C, Eter N. Subretinal drusenoid deposits associated with pigment epithelium detachment in age-related macular degeneration. *Retina*. 2012;32:1727–1732.
51. Sassmannshausen M, Pfau M, Thiele S, et al. Longitudinal analysis of structural and functional changes in presence of reticular pseudodrusen associated with age-related macular degeneration. *Invest Ophthalmol Vis Sci*. 2020;61:19.
52. Reiter GS, Told R, Schranz M, et al. Subretinal drusenoid deposits and photoreceptor loss detecting global and local progression of geographic atrophy by SD-OCT imaging. *Invest Ophthalmol Vis Sci*. 2020;61:11.
53. Wightman AJ, Guymer RH. Reticular pseudodrusen: current understanding. *Clin Exp Optom*. 2019;102:455–462.
54. Querques G, Canoui-Poitrine F, Coscas F, et al. Analysis of progression of reticular pseudodrusen by spectral domain-optical coherence tomography. *Invest Ophthalmol Vis Sci*. 2012;53:1264–1270.
55. Xu X, Liu X, Wang X, et al. Retinal pigment epithelium degeneration associated with subretinal drusenoid deposits in age-related macular degeneration. *Am J Ophthalmol*. 2017;175:87–98.
56. Ayyagari R, Mandal MN, Karoukis AJ, et al. Late-onset macular degeneration and long anterior lens zonules result from a CTRP5 gene mutation. *Invest Ophthalmol Vis Sci*. 2005;46:3363–3371.
57. Mandal MN, Vasireddy V, Reddy GB, et al. CTRP5 is a membrane-associated and secretory protein in the RPE and ciliary body and the S163R mutation of CTRP5 impairs its secretion. *Invest Ophthalmol Vis Sci*. 2006;47:5505–5513.
58. Chavali VR, Khan NW, Cukras CA, Bartsch DU, Jablonski MM, Ayyagari R. A CTRP5 gene S163R mutation knock-in mouse model for late-onset retinal degeneration. *Hum Mol Genet*. 2011;20:2000–2014.
59. Cukras C, Flamendorf J, Wong WT, Ayyagari R, Cunningham D, Sieving PA. Longitudinal structural changes in late-onset retinal degeneration. *Retina*. 2016;36:2348–2356.
60. Suzuki M, Sato T, Spaide RF. Pseudodrusen subtypes as delineated by multimodal imaging of the fundus. *Am J Ophthalmol*. 2014;157:1005–1012.
61. Jacobson SG, Cideciyan AV, Wright E, Wright AF. Phenotypic marker for early disease detection in dominant late-onset retinal degeneration. *Invest Ophthalmol Vis Sci*. 2001;42:1882–1890.
62. Gliem M, Muller PL, Mangold E, et al. Sorsby fundus dystrophy: novel mutations, novel phenotypic characteristics, and treatment outcomes. *Invest Ophthalmol Vis Sci*. 2015;56:2664–2676.
63. Christensen DRG, Brown FE, Cree AJ, Ratnayaka JA, Lotery AJ. Sorsby fundus dystrophy—a review of pathology and disease mechanisms. *Exp Eye Res*. 2017;165:35–46.
64. Burstedt MSI, Ristoff E, Larsson A, Wachtmeister L. Rod–cone dystrophy with maculopathy in genetic glutathione synthetase deficiency. A morphologic and electrophysiologic study. *Ophthalmology*. 2009;116:324–331.
65. Aleman TS, Cideciyan AV, Sumaroka A, et al. Retinal laminar architecture in human retinitis pigmentosa caused by Rhodopsin gene mutations. *Invest Ophthalmol Vis Sci*. 2008;49:1580–1590.
66. Hood DC, Lazow MA, Locke KG, Greenstein VC, Birch DG. The transition zone between healthy and diseased retina in patients with retinitis pigmentosa. *Invest Ophthalmol Vis Sci*. 2011;52:101–108.
67. Lima LH, Cella W, Greenstein VC, et al. Structural assessment of hyperautofluorescent ring in patients with retinitis pigmentosa. *Retina*. 2009;29:1025–1031.
68. Schuerch K, Woods RL, Lee W, et al. Quantifying fundus autofluorescence in patients with retinitis pigmentosa. *Invest Ophthalmol Vis Sci*. 2017;58:1843–1855.
69. Robson AG, Tufail A, Fitzke FW, et al. Serial imaging and structure-function correlates of high-density rings of fundus autofluorescence in retinitis pigmentosa. *Retina*. 2011;31:1670–1679.

Investigative Ophthalmology & Visual Science